XVII IMEKO World Congress
Metrology in the 3rd Millennium
June 22–27, 2003, Dubrovnik, Croatia

ABSOLUTE DISTANCE MEASUREMENT WITH MINIATURIZED FIBER-OPTIC WHITE LIGHT INTERFEROMETER

Christof Bosbach, Tilo Pfeifer, Frank Depiereux

Fraunhofer IPT, Dept. Metrology and Quality Management, Aachen, Germany

Abstract – White light interferometry or coherence radar is a well known and established measurement technique for years. But especially the field of production technology and medical technology need measurement systems with continuously increasing performance. This paper demonstrates, how the use of special optical components for higher measurement frequencies and the miniaturizing of the sensor tip can enlarge the application fields for this system. First, the fundamental aspects of white light interferometry are presented and lead to the new concept of a distance measurement system. It is shown how the inset of a special stepped mirror in the detection interferometer increases the measurement frequency and how the sensor is miniaturized using a Fabry-Perot interferometer.

Keywords: white-light interferometer, miniaturization, distance measurements

1. PROBLEM

The focus of the BmBF-funded research project "DISTANCE" was the development of a distance measuring system, which would permit measuring operations to be conducted in cavities with a diameter of less then one millimeter. Other development objectives arising from the need for miniaturization are as follows:

- miniaturized, freely positionable sensor tip ,
- large measuring range in relation to the parts to be measured,
- ability to work at a relatively high measuring frequency and
- a high level of system independence from, and imperviousness to environmental influences.

Due to the characteristics of the fiber-based systems, these are the ones most likely to achieve the required level of miniaturization (sensor tip diameter 1mm). It is very convenient that a transmitter or sensor unit and a receiver unit can be set up in isolation from one another and that the signals are transmitted via fibers. Consequently, the function of the sensor can be restricted to emitting and receiving the signal (Fig. l). Orientation parameters have been defined for the measuring system in addition to the requirements which have so far tended to be expressed in rather general terms (Table 1).

Characteristic	Value
Measuring distance	0,9mm
Measuring range	0,8mm
Length of sensor shaft	30mm
Diameter of sensor tip	~1mm

TABLE 1**:** Characteristic values for the distance sensor

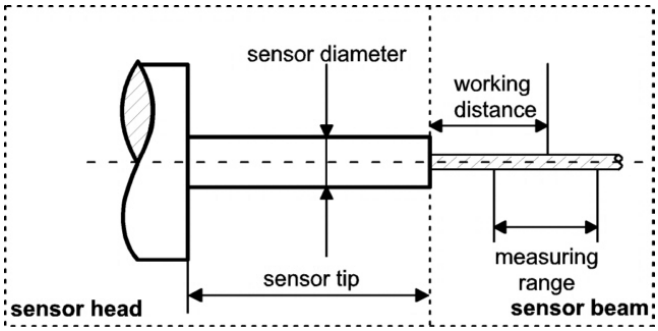

FIG. 1**:** Basic sensor design

The requirements formulated, form the basis for the selection of a suitable measuring technique. It is vital to select a principle/method which is as robust as it is easy to handle.

2. WIDELY USED MODULATION PRINCIPLES

In optical measuring technology, light is always used as an immaterial means for measurement purposes. Depending on the measuring principle applied, the quantity concerned is measured either directly or indirectly. In the case of fiber-optic sensors, the factors which can influence the light, are based on the following types of modulation:

- Intensity modulation
- Phase modulation
- Frequency and wavelength modulation

Closer examination of the various measuring principles and the types of modulation on which they are based, indicates that frequency and wave length modulation provide a suitable means of meeting the requirements of a

micro-sensor specified in the description of the problem. The special feature of this type of modulation is the spectral measurement signal coding. Consequently, the sources of faults arising from fiber quality or external (mechanical) influence, is negligible. The theoretical foundations of frequency and wave-length modulation, are therefore examined in greater detail in the following chapter.

3. FIBER-BASED WHITE LIGHT INTERFEROMETRY

3.1. Spectral Coding

The basic transmission of specially coded measured values is illustrated in Fig. 2. The power density spectrum of a broadband light source, characterized by the wave length λ, is fed into a fiber. The transmitter is described as a spectral filter by the transmission function TG, depending on the measured value (or distance value) x.

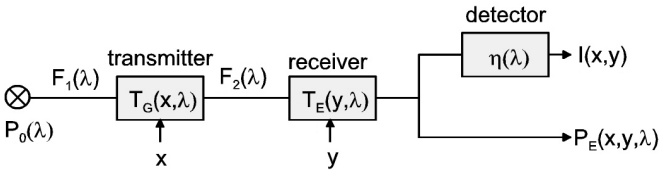

FIG. 2**:** Transmission of a spectrally coded measurement value x

Functions F1 and F2 describe the transmission function of the fibers which, just like the power density spectrum of the source P0 , can be regarded as constant. This also applies to the quantum efficiency η of the detector, which is dependent on wave length. There is a signal at the exit point of the transmitter, which is dependent only on the measured value x and wave length λ. In other words, the measurement value x is coded in the signal. . The transmission function TE of the receiver, depends only on Value y, which is the same type of physical variable as x and whose value usually differs from that of x. The following applies to the detector signal I:

$$P(\lambda) = F_1(\lambda)^2 \cdot F_2(\lambda)^2 \cdot \eta(\lambda) \cdot P_0(\lambda) \tag{1}$$

$$I(x,y) = \int_0^\infty T_G(x,\lambda)^2 \cdot T_E(y,\lambda)^2 \cdot P(\lambda) \cdot d\lambda \tag{2}$$

Where it can be assumed that P is constant in a system set-up, the detector signal I depends only on the values x and y. Here, damping, chromatic dispersion and mode dispersion thus have no influence on the outcome. Changes in the transmission behavior of the fibers can be regarded as variations in the basic spectrum of the light source, as long as they are independent of measured variable x. These characteristics are vital to the reliability of spectral measured value coding.

3.2 Describing in the time domain

As previously outlined, the conversion of fiber-based white light interferometry is based on the combination of a transmitter and a receiver interferometer. The principal demand in relation to the transmitter interferometer is that it can be miniaturized. The principle of the Fabry-Perot interferometer is a suitable set-up for this purpose. Since there are no restrictions on the receiver interferometer, a Michelson interferometer is used as a basis in this case (Fig. 3).

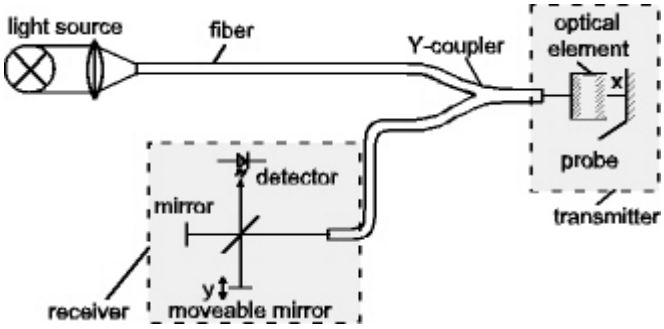

FIG 3: Double interferometer set-up

In the set-up presented here, the path difference, i.e. the measured value, is coded by the signal using a semi-reflecting optical element. This is achieved by first de-coupling the signal from the broadband light source from the fiber. The light is divided into a reference beam and a measuring beam in the optical element. The reference beam is immediately lead back into the fiber as the reference wave. The measurement beam exits the optical element and is reflected by the surface of the object to be measured.. Depending on the quality of the surface of the object, the optical element may lead some of the reflection back into the fiber in the form of a wave package.)

The Michelson-Interferometer receiver can be regarded as a transverse filter, which splits the input signal into two signals, each with half power and superimposes them again with a time delay, in the detector. The delay is set via the (mechanically) movable mirror. It is essential to formulate the electrical field E of the stochastic radiation source in dependence on the time t, before the time domain can be examined and before the intensity signal can be calculated. Thus a total of four signals are superimposed on one another in the detector; The input signal E(t) and the signals delayed by τ_i :

$$\tau_1 = t + \frac{x}{c}, \quad \tau_2 = t + \frac{y}{c}, \quad \tau_3 = t + \frac{x+y}{c} \tag{3}$$

Since the origin of the delayed signals is the same, it is possible to describe them in terms of their auto-correlation function [7], which also provides the measure of the time coherence. Detector signal 1 is given by the sum of the auto-correlation functions:

$$I(x,y) \approx \frac{1}{2T} \sum_n \int_{-T}^{T} E(t) \cdot E(\tau_n) \cdot d\tau \tag{4}$$

The integration time T, is long in comparison with the frequencies of the optical signal.

3.3 Determining the transmission functions

The effect used in the transmitter interferometer to divide the beam into a reference and a measuring part, is based on the Fresnel reflection. This means that reflection occurs due to the difference in density at the point of transition from the optical element to air. Glass reflection is in the order of approx. 4 % to 6 % of the total intensity, depending on the gradient of the density difference. The amount of the light which actually hits the measurement object, is therefore between 94% and 96%. Utilization of the Fresnel reflection also means that the optical element in the system equipment does not have to fulfil any particular specifications and that a GRIN lens can be used. At the same time, the GRIN-lens collimates the beam. This is essential because of the numerical fiber aperture.

The transfer functions U_E and U_G can be formulated on the basis of the interferometer types selected for the receiver and the transmitter. The transfer function for the receiver, can be developed using the series expansions from (1) and (2) to form the following function:

$$T_E(y,\lambda)^2 = \tfrac{1}{2}\left(1+\cos\left(\frac{2\pi\cdot y}{\lambda}\right)\right) \qquad (5)$$

The transfer function of the transmitter can be deduced from the known Airy-Function [8], in which here, the amplitude transmission coefficient T_{Obj} on the object side is specified as zero (Fig. 4). The variables R_i represent the reflection coefficient of the amplitude of the GRIN lens and of the object to be measured. As in previous references, typical values for the transition from glass to air are R_{Sp}= 0.2 (corresponding to 4%) and T_{Sp}=0.8. In developing the transmission function of the transmitter, no account has been taken of the dispersion effects or of the occurrence of an evanescent wave in the object:

$$T_G(x,\lambda)^2 = \frac{\left(R_M - R_{Obj}\right)^2 + 4\cdot R_M\cdot R_{Obj}\cdot\sin^2\left(\frac{2\pi\cdot x}{\lambda}\right)}{\left(1-R_M\cdot R_{Obj}\right)^2 + 4\cdot R_M\cdot R_{Obj}\cdot\sin^2\left(\frac{2\pi\cdot x}{\lambda}\right)} \qquad (6)$$

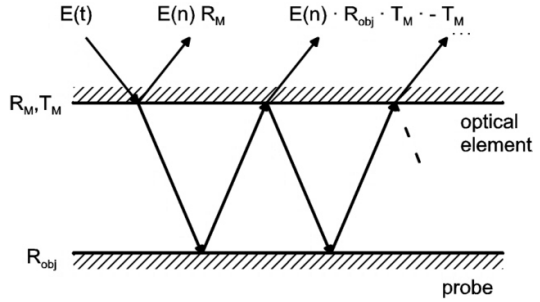

FIG. 4: Reflections in a Fabry-Perot Cavity

Assuming that the light source has a gaussian power density spectrum, a typical interferogram or correlation diagram is produced when the transmission functions are inserted into (2) (Fig. 5). The number of secondary signatures arising from the multiple reflection within the Fabry-Perot cavity, which is theoretically possible, is striking. In practice, only the first secondary signature (left and right) becomes clearly visible in addition to the main signature. This is also expressed in the so called Finesse calculated, which reaches a maximum value of only 1.6 given the parameters concerned here (Fresnel-Reflection and engineering surface). Multiple reflections within the Fabry-Perot cavity are therefore suppressed and only the first secondary signature develops.

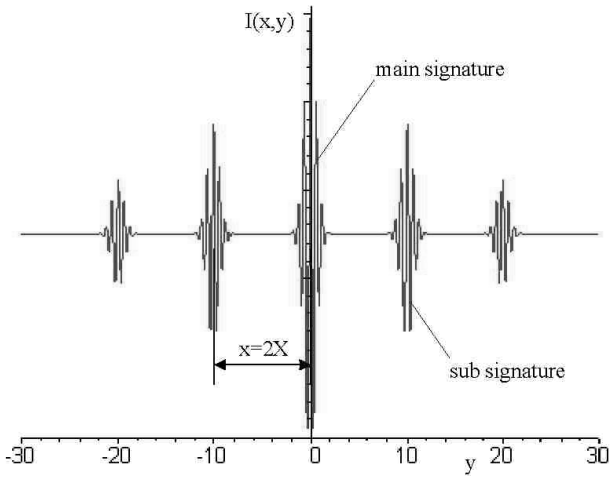

FIG. 5**:** Interferogram with several sub-signatures

4. SYSTEM DESIGN

Having completed the theoretical investigation of fiber-based white light interferometry, attention must now turn to system design. One of the particular drawbacks of the interferometric systems used to date, is the need to tune the measurement range mechanically using a mirror, in order to determine the measurement result. The speed at which this is carried out, can be increased significantly only when all parts or assemblies which are moved mechanically, have been eliminated. One aim, therefore, is to achieve electronic tuning of the measurement area. A further aim is to miniaturize the transmitter interferometer in accordance with the requirements which have been specified.

4.1. Development of a stepped mirror

The stepped mirror is the central element in any operation to scan the area to be measured electronically. The function of the stepped mirror will be explained on the basis of one individual step. The function of one individual step in the stepped mirror, is illustrated clearly in Fig. 6. The beam emitted by the fiber is first collimated by an expansion lens in the receiver interferometer, which fully illuminates the step. The wave packages, with a time lag of τ to τ_1 , corresponding to a distance of 2x from the object to be measured, are split by the beam splitter in both directions as previously described. The surface normal line of the step is set at a defined angle θ to the angle of incidence. This compensates for the path difference of x. Since the distance from the measurement beam to the object to be measured is covered twice (there and back) by the transmitting interferometer, the path between the beam splitter and the

stepped mirror must likewise be covered twice by the wave package, for decoding purposes.

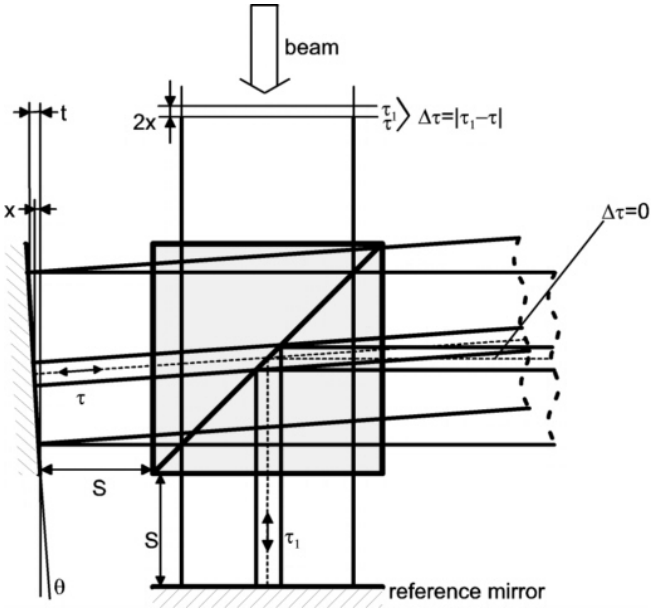

FIG 6**:** Functional principle of a single step

The maximum path to be compensated, is described by the step depth t. This permits the measuring range to be can be selected within wide limits, by combining several steps. The step depth selection is limited by the maximum permissible angle θ, the radiation source concerned and by the detector, which is being used. A stepped mirror with the values for the actuation distance and measuring range listed in Table 1, is shown in Fig. 7.

4.2. Selecting a radiation source

In practice, the surfaces encountered are likely to be rough in engineering terms. This means that the measuring system must not react sensitively to differences of several micrometers in height. However, when surface roughness reaches a level at which the wave packages reflected from the uppermost surface structures can no longer interfere with the wave packages reflected from the lower structures, the coherence length of the radiation source is too small. Since the interactions which occur are very complex, an approximation (7) was developed from [9] to cover this aspect. In this approximation, the coherence length l_C is set in relation to the surface roughness σ_Z . The coherence length l_C is the ratio of mean wave length λ_0 and the spectral width $\Delta\lambda$ of the radiation source. It is important to observe this ratio, since the visibility of the secondary signature to which reference has previously been made, diminishes to an unacceptable level.

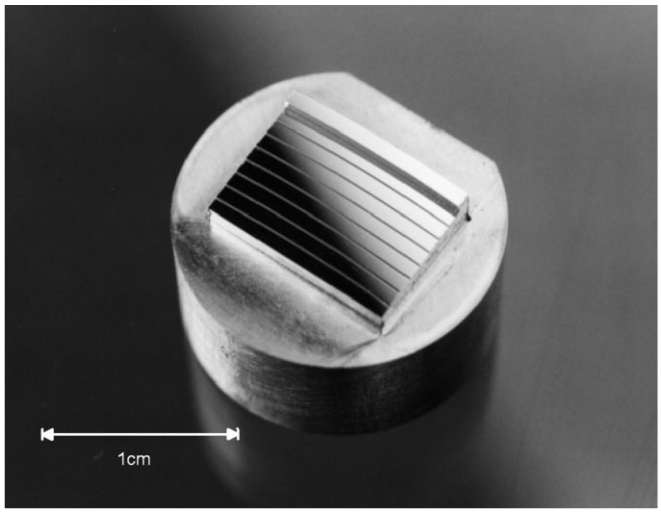

FIG.7: Stepped mirror

$$l_c = \frac{\lambda_0^{\,2}}{\Delta\lambda} \le \frac{4\cdot\pi}{\sqrt{2}}\cdot\sigma_z \qquad (7)$$

Short-coherence radiation sources which produce a particularly precise interferogram with pronounced main and secondary signatures in accordance with (2), have the disadvantage of excessively short coherence. A typical short-coherence thermal radiation emitter with a coherence length of approx. $l_C=5\mu m$ begins to suffer from a significant loss of visibility of the interferogram at a surface roughness level of just over $\sigma_z=0.6\mu m$. Consequently, it is impossible to record measurement values for a number of engineering surfaces using thermal radiation. The application of a source with a coherence length of approx. $l_C=48\mu m$ increases the value to $\sigma_z=5{,}8\mu m$.

4.3 Sensortip design

In principle, the transmitter interferometer, or sensor tip, consists of only a fiber, which is fed in a glass tube and the optical element, the GRIN lens mentioned previously. The sensor tip consists of a 0.5 mm glass tube with a centered 128µm long through-hole. A mono-mode fiber with an external diameter of 125 µm is pushed through this hole and bonded into the glass tube . The GRIN lens is glued on top of the tube. The complete sensor finger with a shaft of 30 mm in length, is shown in Fig. 8.

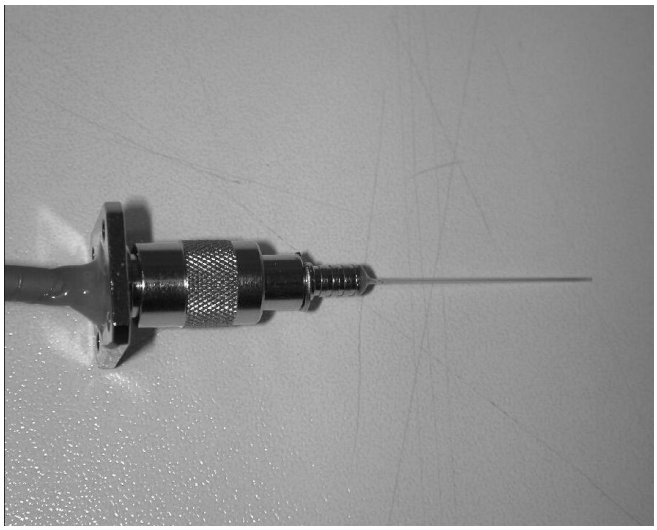

FIG. 8: Assembled sensor head

5. TEST RESULTS

The orientation of the stepped mirror in conjunction with the light source used, results in a signature which extends over parts of the step, with maximum intensity in the middle of the signature. This behavior is demonstrated by the example of the main signature in Fig. 9. The diagram shows the detector image available for evaluation in the receiver-interferometer.

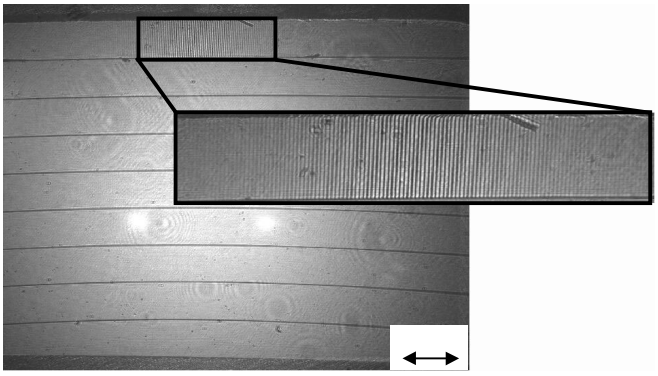

FIG. 9: Position of the main signature

Two different sample surfaces were used to test the sensor. The sample surfaces differ in terms of their roughness and in their amplitude reflection co-efficient. Tests were conducted on a polished steel surface and on a steel surface which had been machined using mechanical methods. This involved the use of a positioning table to position the sensor above the sample. The sensor was then moved as required. The inclination of the samples were movable, in order to ensure that the angular sensitivity of the sensor could be measured. The measurement results are shown in Figs 10-11. The diagrams have been standardized in order to facilitate comparison. This was done by using the predominant Fresnel reflection in the detector interferometer, which is independent of the sample, as a basis and by setting it in relation to the input intensity in the receiver interferometer during the measuring operation.

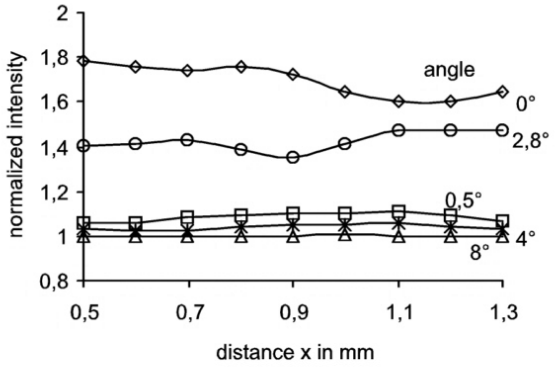

FIG. 10: Measurement operations conducted on steel machined using mechanical methods

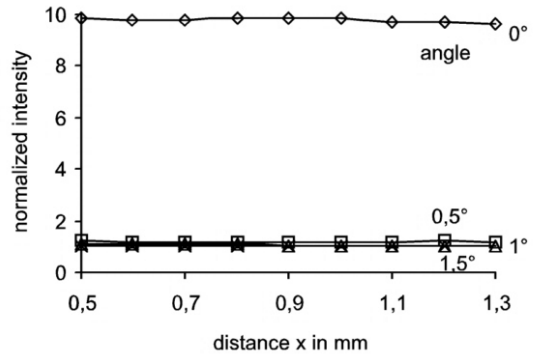

FIG. 11: Measurement operations conducted on polished steel

As these diagrams demonstrate, the sensor is capable of recording measured values on both test surfaces. However, the differences in the inclination characteristics and the different levels of intensity are striking. In the case of measuring operations conducted on steel which has been machined using mechanical methods, it is apparent that measuring operations can be conducted up to a surface angle of inclination of 8°. Additionally, the intensity of the beam returning from the surface of the test parts is so weak that it is no longer possible to detect any auxiliary signatures on the detector image. It is also apparent from the diagram that the mean level of intensity does not diminish at a constant rate as the angle of inclination increases. In fact, there is a considerable amount of fluctuation. This fluctuation is due to the surface structure of the sensor. Overall, the measuring system proves to be highly suitable for this application.

It is to be expected that there will be a considerable change in the reflection lobe of the sensor surface when the measuring operation is conducted on polished steel as opposed to steel which has been machined using mechanical methods. A glance at the diagram (Fig. 11), confirms that this is, indeed, the case. When the sensor orientation is normal to the surface of the sensor, there is a considerable increase in the mean intensity level. This indicates that the reflection is virtually specular. This assumption is confirmed

by further measurement. Since the level of angle sensitivity is very high, the maximum is reached at an angle of inclination of 1.5°.

6. SUMMARY

Given the level of technology currently available, the requirements to be met by a miniaturized distance measuring system, can be met only by fiber-optic systems. White light interferometry, which permits absolute distance measurement and which has does not react readily to ambient influence due to the spectral coding of the measurement signal, is the preferred measuring principle. It is vital to use a double interferometer construction consisting of a Fabry-Perot interferometer (detector) and a Michelson interferometer (receiver) in order to miniaturize the system, particularly the sensor tip.

The use of a special, stepped mirror permits an electronic scanner to be implemented in the receiver interferometer. This makes it possible to record the entire measuring area without any need for elements which are moved mechanically and to achieve high measuring frequencies. The design of the transmitting interferometer was restricted to the elementary functions, thus permitting a GRIN lens to be used to collimate the beam at the point of fiber exit.

The measurement results show that the sensor can carry out a wide range of measuring operations, despite its angular sensitivity. The fact that it is not influenced by various test surfaces, demonstrates that the measuring principle meets the requirements specified.

Acknowledgement

The results presented in this article were obtained in the course of the "DISTANCE" project. The project was funded by the BMBF as part of the "Micro-Systems Technology 2000 +" support program. The other partners in the collaborative project were the companies CeramOptech GmbH, Bonn, Jurca GmbH, Rodgau and OKM GmbH in Jena.

REFERENCES

[1] *T. Pfeifer* und *E. Eikelmann***:** Fiber-optic reflex sensors for industrial applications. Measurement 12 (1994), S. 291-304

[2] *Y. Yang, K. Yamazaki, H. Aoyama* und *S. Matsumiya***:** Fiber optic surface measurement sensor and its design study. Precision Engineering 24 (2000), S. 32-40

[3] *W. Bludau:* Lichtwellenleiter in Sensorik und optischer Nachrichtentechnik. Springer Verlag Heidelberg 1998

[4] *R. A. Jarvis***:** A Laser Time-of-Flight Range Scanner for Robotic Vision. IEEE Trans Pattern Anal. Machine Intell. PAMI-5 (1983), S. 505-512

[5] *P. Ettl, P. Habermeister* und *G. Häusler***:** Kohärenzradar – ein 3D-Sensor im Genauigkeitsbereich von 1µm. Technisches Messen No. 67 (2000), S. 52-57

[6] *C. Bosbach, S. Driessen, T Pfeifer* und *B. Michelt***:** Fiber-optic interferometer for absolute distance measurements with high measuring frequency. Proceedings of 2nd euspen International Conference, Turin (2001), s. 278-281

[7] *H. S. Lipson, G. Lipson* und *D. S. Tannhauser***:** Optik. Springer-Verlag, Berlin (1997), ISBN 3-540-61912-7

[8] *D. Miller***:** Refractive Fabry-Perot bistability with linear absorption: Theory or Operation and Cavity Optmization. IEEE Journal Of Quantum Electronics, VOL. QE-17, No. 3 (1981), S. 306-311

[9] *N. George***:** Speckle at various Planes in an optical System. Optical Engineering, Vol. 25, No. 6 (1986)

Autoren: Prof. Dr.-Ing. T.-Pfeifer, Dipl.-Ing. C. Bosbach, Dipl.-Ing. F. Depiereux, Fraunhofer Institut für Produktionstechnologie IPT, Steinbachstr. 17, 52074 Aachen, EMail: c.bosbach@ipt.fraunhofer.de, Tel.: +49 241 8906 113